Near Infrared Spectra of 12 Near Earth Objects

John K. Davies[1], **Alan W. Harris**[2], **Andrew S. Rivkin**[3], **Stephen D. Wolters**[4], **Simon F. Green**[4], **Neil McBride**[4], **Rita K. Mann**[5], and **Tom H. Kerr**[6]

[1] UK Astronomy Technology Centre, Blackford Hill, Edinburgh, EH9 3HJ, UK. e-mail jkd@roe.ac.uk

[2] DLR Institute of Planetary Research, Rutherfordstrasse 2, 12489 Berlin, Germany.

[3] Applied Physics Laboratory, Johns Hopkins University, Baltimore, USA.

[4] Planetary and Space Science Research Institute, The Open University, Walton Hall, Milton Keynes, MK7 6AA. UK.

[5] Institute for Astronomy, 2680 Woodlawn Dr, Honolulu, HI, 96822, USA.

[6] Joint Astronomy Centre, 660 N A'ohoku Pl., Hilo, HI 96720, USA.

44 Pages

14 Figures

3 Tables

Running Head Near-IR Spectra of 12 NEOs

Address for correspondence John Davies, UK Astronomy Technology Centre, Blackford Hill, Edinburgh, EH9 3HJ, UK. e-mail jkd@roe.ac.uk

Abstract.

We present a number of spectra of Near Earth Objects taken in the period 1998-2003 with two different instruments (CGS4 and UIST) on the UKIRT telescope. Since observations with CGS4 require multiple spectral fragments to be observed sequentially and then spliced together we assess the reliability of this technique using comparisons between multiple observations of the same object, between observations of the same object with both instruments and with independent spectra of common objects. We conclude that while problems in the spectral splicing can occur, they are usually intuitively obvious and that overall our dataset is sound. The objects for which we present new spectral data are: 1627 Ivar, 4179 Toutatis, 5381 Sekhmet, (5587) 1990 SB, 6489 Golevka, (11405) 1999 CV_3, (14402) 1991 DB, 25143 Itokawa, (25330) 1999 KV_4, (52760) 1998 ML_{14}, (66391) 1999 KW_4, and (101955) 1999 RQ_{46}. Our results, together with albedo data from the literature, suggest carbonaceous compositions for 25330 and 101955. The available data for 14402 suggest it may belong to the relatively rare M class. Our analysis suggests an S or Sq classification for 52760 and a V classification for 5381 Sekhmet. For all remaining objects the UKIRT data are consistent with published spectral classifications. We find that only 3 of the 12 objects are not S/Q/V-class, which is roughly consistent with the results of Binzel et al (2004, Icarus, 170, 259-294). Four spectra of Toutatis taken over a range of solar phase angles between 0.7–81 degrees and at intervals of several weeks are indistinguishable within the uncertainties and therefore do not reveal any evidence for phase reddening or surface variegation.

Keywords Asteroids; Infrared Observations; Spectroscopy.

1 Introduction

Near Earth Objects (NEOs) provide vital clues towards our understanding of how the solar system formed and evolved. They provide a direct link between meteorites, whose study in terrestrial laboratories has given important insights into parent-body processes, and main-belt asteroids, which still occupy positions close to where they were formed. The short dynamical lifetimes of NEOs requires resupply from the main asteroid belt. Binzel et al. (2004) used the spectral properties of NEOs to help constrain the relative proportions of their source regions in the main belt. This knowledge can, in turn, be used to improve the understanding of the processes which bring objects into planet-crossing orbits. The fraction of NEOs which originate from cometary, rather than asteroidal, sources is also important as much of the Earth's water may have arrived via impacts of asteroids or comets. Finally, physical information is a prerequisite for developing adequate deflection strategies for use against an NEO that proves to be a direct threat to the Earth.

There are almost 4000 NEOs now known and this number is steadily increasing. However due to their small size, and hence intrinsic faintness, most objects are only observable for very short periods at long and irregular intervals. Although broadband photometric observations allow objects to be classified into various taxonomic schemes, linking these taxonomies to specific minerals requires spectroscopic observations which can then be used to search for meteoritic analogues and clarify the links between main belt asteroids, NEOs and meteorites.

Therefore we took the opportunity to observe 12 objects when they made close approaches to the Earth during the period from 1998 to 2003. In some cases these were apparitions of known objects which could be planned for, in others they were targets of opportunity; newly discovered objects which were observed during their discovery apparition at short notice and with little or no observing flexibility.

2 Observations

The observations presented here were made over a period of several years using the two common user (facility) instruments on the 3.8m United Kingdom Infrared Telescope (UKIRT) on Mauna Kea, Hawaii. The majority were done with the cooled grating array spectrometer, CGS4, until this instrument was largely replaced by the UIST imager/spectrometer in 2003.

2.1 CGS4

CGS4 was the common user facility spectrometer at UKIRT for over a decade and has been used by us and many others for a series of important solar system observations so the instrument and its reduction proceedures are well described elsewhere. For the observations reported here CGS4 was equipped with its 75 lines/mm grating and its short focal length camera. In this configuration CGS4 has a pixel size of approximately 1.23 by 1.23 arcsec and a slit length of 90 arcsec on the sky.

In first order, the spectral grasp of CGS4 in this configuration is 0.66μm per grating setting. This allows full coverage of either the H or K window, with some extension into the adjacent window if desired. However, the efficiency of the grating falls rapidly at shorter wavelengths and observations in the I or J windows are normally done in second order. Unfortunately this has the unwanted effect of reducing the spectral grasp to 0.33μm per grating setting. The implications of this on our observing and data reduction strategy are given in the following section.

When observing, the spectra were sampled twice per resolution element, and the detector was stepped over two pixels to ensure full spectral coverage in the presence of any bad pixels. Observations were generally made with a 2 pixel wide slit to maximise photometric reliability, although accurate spectrophotometry was not attempted.

Object-sky pairs of observations were made with the telescope being nodded along the slit between observations. The amplitude of this nod was typically 25 rows (approx 30 arcsec). The object and sky frames were differenced and the differences co-added to form a final frame containing two sky-subtracted asteroid spectra. On-chip single exposure times varied from 12 to 20 seconds in the J,H and K bands.

By their very nature NEO observation windows are ephemeral and often occur at short notice as newly discovered objects become available for a short period within a few days of their discovery. Therefore a number of the observations reported here were done in service or other non-PI modes where the authors did not have full control over the observing parameters. Typical settings used during the programme are given in Table 1 although they may have varied slightly on different nights depending on the other observation programmes taking place at the time.

Setting Label	Central wavelength of window (μm)	CGS4 Min (μm)	CGS4 Max (μm)	Comment
K	2.2	1.88	2.52	Includes long end of H window.
H	1.65	1.44	2.08	Includes overlap with K and J_{long}.
J_{long}	1.25	1.24	1.56	
J_{short}	1.25	0.99	1.31	Limited overlap with J_{long}.
I	0.9	0.78	1.1	Rarely used.

Table 1: Table 1. Typical CGS4 spectral ranges used.

Comparison spectra were taken of solar type stars, usually of spectral types between G0V and G5V, at airmasses that matched those of the asteroid as closely as possible. Division of the asteroid spectrum by that of the ratio star thus served both to remove telluric features and produce a reflectance spectrum directly. The use of direct solar analogs, such as 61 Cyg B, although desirable was not generally possible due to the need to match airmasses closely for the best possible removal of telluric features. When possible, two solar type stars were observed so that intercomparisons could be used to identify any effects due to the ratio star. Such effects were generally found to be negligable (ie ratios of the two solar analogue stars did not have a slope or other unexpected spectral features).

A complete observing sequence of calibration arcs, asteroid and ratio star observations for a sequence of 4 grating settings would take 2–4 hours, depending on the brightness of the target asteroid.

2.2 UIST

UIST is a new facility class near-IR (1–5μm) imager and spectrometer at UKIRT which uses a 1024×1024 InSb array plus various grisms and IFU combinations to cover the 1-5μm range. For the asteroid observations presented here, which took place in a single observing run during May 2003, the HK grism was used, giving a spectral coverage of 1.4–2.5μm with a spectral resolution of 800–1000. The JH grism, although installed in the instrument, was not useable during the observing run due to technical issues, restricting our coverage to the 1.4-2.5μm region. Our observing strategy with respect to ratio stars etc was the same as with the earlier CGS4 observations.

3 Production of the Composite Spectra.

In asteroids, the mineralogical spectral features of interest are broad and only obvious when there is wide spectral coverage. In the case of CGS4 the relatively narrow spectral grasp of a single grating setting made it necessary to cover the 1–2.5μm region stepwise in several settings and then splice the spectral fragments together. While conceptually simple, in practice this is a proceedure which has several potential difficulties. For example, the object will be rotating which will cause its brightness to vary with time. The close approach to Earth and consequent change in phase angle may cause it to present different aspects if the observation period extends over several days. It may also be a binary.

From a data reduction perspective one would like considerable overlaps in wavelength between the spectral fragments to maximise the opportunities to normalise them, but excessive overlapping requires extra grating positions which increases overheads. This is particularly acute when dealing with the I /J region, since the need to work in second order reduces the available spectral grasp per setting and requires more observations to cover the required range. These extra overheads make maintaining the asteroid to ratio star airmass match difficult. Good airmass matching is important since the transmission profiles at the edges of the atmospheric windows are steep and spurious spectral slopes can be introduced if the airmasses are not well matched. Rapid airmass changes are particularly problematic when observations are made at large zenith distances and so whenever possible we observed the objects around the time of transit, but naturally this was not always achievable. The atmospheric absorptions also drastically reduce signal to noise in the regions at the edges of the transmission windows which are often precisely the regions where reliable data are needed for the spectral fragment matching.

It is also of note that when ratioing with a star, small changes in the wavelength dispersion, perhaps introduced by instrumental flexure, can produce disproportionate changes in the slope of the resulting ratios. To reduce the effects of such a mismatch, the stellar and asteroid spectra were cross-correlated and, if necessary, sub pixel shifts were made before the asteroid-ratio star division was done.

Once the individual spectral fragments have been obtained there are three possible approaches to the spectral slicing problem.

One method is to use curve fitting at the ends of each fragment to extrapolate to the beginning of the next fragment. Although this would be essential if the wavelength overlap between spectral fragment is very small, or non-existent, we have not used this approach.

A second approach is to reduce each spectral fragment independently and then scale them in terms of absolute flux using some independent information, such as photometry, before adjoining them. While this is a rigourous way of dealing with the problem, and prevents any normalisation errors being propagated along the spectrum, it is often difficult to realise in practice. Modern slit spectrometers do not use apertures large enough to make them good spectro-photometers and so the absolute flux level of each spectral fragment is not well known. The use of broad band photometic measurements can resolve this uncertainty, but only if the photometric data can be taken simultaneously with the spectra so that asteroid rotation does not skew the result. Once again this is difficult to realise since even though UKIRT can mount several instruments simultaneously, switching from the camera to the spectrometer has an overhead of a few minutes which can be significant when the object under study has a rotation period of only a few hours. Furthermore, especially in the case of target of opportunity observations, both instruments may not be available and suitably calibrated on any given night. As a consequence, we used this approach only once, with our observations of 25143 Itokawa.

For the remaining objects we adopted a strategy of maximising the overlap produced by each grating setting, and making some of the common region fall in a zone of good atmospheric transmission. Thus we could select high signal to noise regions clear of the atmospheric window edges which were common to both sub-spectra, take the average values over this region and then factor by multiplication one fragment in such a way as to make it overlay the fragment next to it. We started by normalising the K band spectrum to 1 between 2.15 and 2.25μm, then adjoined subsequent spectra to the left, ie to gradually decreasing wavelengths.

All the data reduction was done using the UKIRT online data reduction package *ORAC-DR* for pipeline operations at the telescope to produce final spectral images. The *STARLINK* package Figaro was used for more detailed operations such as final wavelength calibration, ratioing and spectral splicing.

4 Verification of the Splicing technique.

Given the uncertainties in splicing together up to 5 (I, J_{short}, J_{long}, H and K) spectral fragments is it obviously sensible to compare our results with those obtained in other ways. Fortunately several opportunities to do this do exist.

1) Other instruments such as the cross dispersed SPEX instrument at the NASA InfraRed Telescope Facility (IRTF) and the grism spectrometer SOFI at the European Southern Observatory both provide wide spectral coverage without the need for spectral splicing. Publications resulting from these instruments have allowed us to carry out a comparison of our data with those of other observers in a number of cases where one or more teams observed the same object during the same or different apparitions. In particular we have drawn heavily on the datasets of Binzel et al (2004) and the paper by Lazzarin et al (2004). These data are non-simultaneous with ours and often cover complementary spectral ranges, so we are in the fortunate position that comparisons of the datasets can both verify our splicing process

and at the same time extend the published data to longer wavelengths.

In the case of 6489 Golevka we can compare our observations taken in 1999 with CGS4 over the range 1.15–2.5μm using the splicing technique with our own 2003 observations using the UIST grism in a single exposure covering 1.6–2.5μm (see section 6.5).

Finally, in the case of Toutatis (section 6.2) we have observations on four dates all made with CGS4. Although the objective of these observations was to search for subtle differences in the spectra under different observing geometries, they also provide an opportunity to check for problems in our reduction methodology.

Our conclusion is that in most cases where direct comparisons are possible our spliced spectra are similar in shape to those from other workers. Furthermore, where inconsistencies do emerge, they are usually in cases where it is intuitively obvious that something has gone wrong in the reduction process. This gives us confidence that, despite the potential difficulties of spectral fragment splicing, our data reduction technique is not producing major undetected distortions in the overall spectral shape we derive. In the following section we present the results for each object observed, plus any specific comments on the technical issues surrounding the data and some brief conclusions based on our spectra.

5 Observation Summary

Target Name	Date	R (AU)	δ (AU)	Phase Angle (deg)	V Mag	Lambda Range (μm)	No of Grating Settings	Ratio Star
1627 Ivar	2000 Mar 12	2.075	1.089	4.92	15.2	1.25–2.5	3	BS4437
4179 Toutatis	2000 Dec 01	0.997	0.187	81.0	14.6	1.2–2.5	3	BS4437
4179 Toutatis	2000 Dec 22	1.138	0.269	49.1	14.7	1.0–2.5	4	BS4437
4179 Toutatis	2001 Jan 14	1.329	0.372	18.6	14.8	1.0–2.5	4	BS3510
4179 Toutatis	2001 Feb 01	1.487	0.502	0.7	14.8	1.0–2.5	4	BS3510
5381 Sekhmet	2003 May 05	1.087	0.206	62.4	15.5	1.4-2.5	1	BS7260
5381 Sekhmet	2003 May 07	1.095	0.186	58.0	15.1	1.4-2.5	1	BS7260
5587 1990 SB	2001 Mar 31	1.465	0.518	21.0	14.0	0.80–2.5	5	BS5384
6489 Golevka	1999 May 19	1.053	0.051	38.6	14.4	1.14–2.42	3	BS6060
6489 Golevka	1999 Jun 8	1.029	0.059	74.5	15.7	1.9–2.5	1	BS8314
6489 Golevka	2003 May 11	1.103	0.113	33.0	16.1	1.4–2.5	1	16 Cyg B
11405 1999 CV_3	1999 Feb 19	1.216	0.236	14.5	13.1	1.15–2.4	3	BS4027
14402 1991 DB	2000 Mar 12	1.089	0.107	26.1	14.9	0.99–2.52	4	BS4437
25143 Itokawa	2001 Mar 17	1.049	0.064	31.4	14.7	0.8–2.5	5	BS5364
25143 Itokawa	2001 Mar 18	1.046	0.061	33.2	14.6	0.8–2.5	5	BS5364
25143 Itokawa	2001 Mar 19	1.042	0.058	35.2	14.5	JHK		Photometry
25330 1999 KV_4	2003 May 06	1.251	0.351	11.0	15.5	1.4–2.5	1	BS5657
25330 1999 KV_4	2003 May 09	1.368	0.362	7.42	15.5	1.4–2.5	1	BS5657
52760 1998 ML_{14}	1998 Aug 11	1.013	0.02	91.4	12.3	1.88–2.5	1	BS1747
52760 1998 ML_{14}	1998 Aug 12	1.008	0.02	104.2	13.2	1.4–2.0	1	BS1532
52760 1998 ML_{14}	1998 Aug 12	1.008	0.02	104.2	13.2	1.9–2.5	1	BS1747
52760 1998 ML_{14}	1998 Aug 13	1.002	0.02	113.9	14.1	1.14–1.45	1	BS1532
52760 1998 ML_{14}	1998 Aug 13	1.002	0.02	113.9	14.1	1.64–2.26	1	BS1747
66391 1999 KW_4	2001 May 29	1.051	0.053	43.7	11.8	0.8–2.5	5	BS5534
101955 1999 RQ_{46}	1999 Sep 22	1.004	0.015	86.7	14.7	1.43–2.52	2	BS2208
101955 1999 RQ_{46}	1999 Sep 22	1.001	0.014	97.8	15.3	1.0–1.55	2	BS2208

Table 2: Table 2. Details of the observations taken. *Note that geometric values are approximate for the mid time of each observing period. The V magnitudes quoted are for illustration and are based upon ephemeris calculations, not actual observations.*

6 Results

6.1 1627 Ivar

This S type object was observed on 2000 March 12. Three grating settings were used providing a good quality spectrum from 1.25–2.5μm. A spectrum from Binzel et al (2004) extends to 1.6μm and the overlap with our data is excellent with only a minor divergence at the extreme short end of our spectrum, between about 1.25 and 1.35μm. In view of this agreement we have combined the two datasets as shown in Fig.1, note that some noisy data in the 1.4-1.5μm region have been removed.

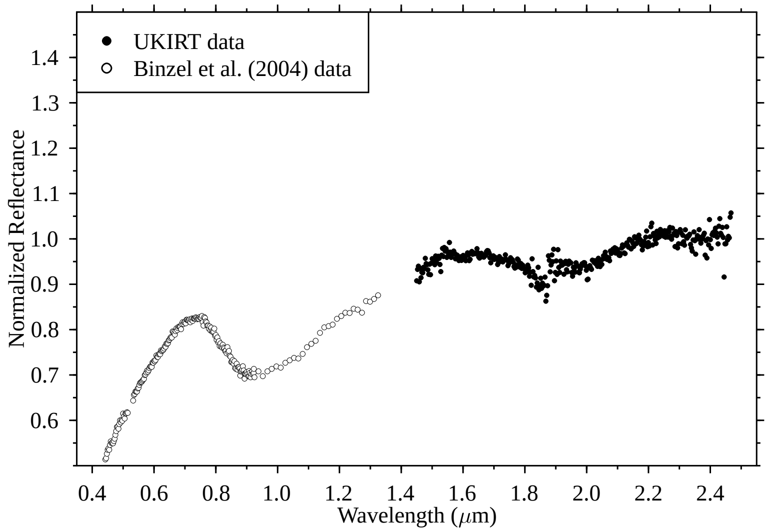

Figure 1: 1627 Ivar. Merger of the UKIRT data with that of Binzel et al (2004).

According to Ostro et al. (1990) and Delbo et al. (2003) the diameter of this S-type Amor asteroid is around 9km, which makes it the largest object in our sample. The albedo derived by Delbo et al. from thermal-infrared observations assuming H = 12.87 is $p_v = 0.15 \pm 0.05$. The value given by Kiselev et al. (1994) from polarimetry is $p_v = 0.14$. The albedo results are consistent with an S-type classification, as are the olivine and pyroxene absorption bands evident in the spectrum.

6.2 4179 Toutatis

This S type object was observed over wide range of wavelengths in January 1993 as described by Howell et al (1994). We chose to re-observe it in 2000-2001 in an attempt to seek evidence for phase reddening, an important phenomenon which could affect the interpretation of asteroid spectra. This effect, which is due to complex multiple scattering in rough surfaces, causes spectral slopes to change as a function of solar phase angle and is therefore particularly relevant to observations of Near Earth Objects which are often observed at large phase angles. Phase reddening is evident in optical spectra, as discussed by Luu and Jewitt (1990) but the extent to which it may affect spectra in the near infrared range is unknown. In late 2000/early 2001 there was a rare opportunity to study this phenomenon using observations of 4179 Toutatis. Over a six week period the object's apparent brightness remained almost constant at around V=14.7 over a very wide range of solar phase angles (0-80 deg.).

Accordingly 4179 Toutatis was observed on four occasions during this period to seek any evidence for phase reddening in the infrared. The four datasets obtained are shown in Fig.2. Observations on 1 December 2000 were limited to three grating settings since the large phase angle meant that the object did not rise until the early hours of the morning and there was insufficient time to obtain all four grating positions before dawn. Our spectra are consistent with those of lower resolution, but greater spectral coverage, presented by Howell et al (1994).

Due to the asteroid's motion across the sky over the 6 week observing period, we were obliged to use two different ratioing stars (BS3510, G1V and BS4437, G0V) since the increasing angular separation of the object from the first ratio star would have made airmass matching impossible towards the end of the observing window. However, on one of the nights midway in the observing period both stars were observed and then ratioed with each other to search for any spectral differences. No such differences were found (i.e. the ratio of the two stellar spectra was flat) and confirming that no anomalous spectral slopes would have been introduced by the use of two different ratio stars.

Although the data has been reconstructed with care it has not been possible to detect any unambiguous phase reddening effects, all four spectra appear identical to within the errors. This remains true even when restricting the analysis to single bands to avoid the uncertaintities associated with spectral splicing. For example, Fig. 3 shows the ratio of the K band reflectance spectrum on 2000 December 01 with that of 2001 February 01. These two observations span a phase angle range of almost 80 degrees and yet the ratio of the two spectra is flat. The ratio has been normalised to 1 at 2.2 μm and the vertical scale is the same as the other plots in the paper to ease comparison. Excessive noise is seen in the regions of poor atmospheric transmission at each end of the spectrum and at around 2.1μm. We have calculated the mean value and standard deviation over three 0.1μm intervals from 2.05-2.15, 2.25-2.35 and 2.35-2.45 μm. These values are respectively 1.002 ± 0.023, 1.020 ± 0.021 and 1.035 ± 0.036, confiming the visual impression of flatness.

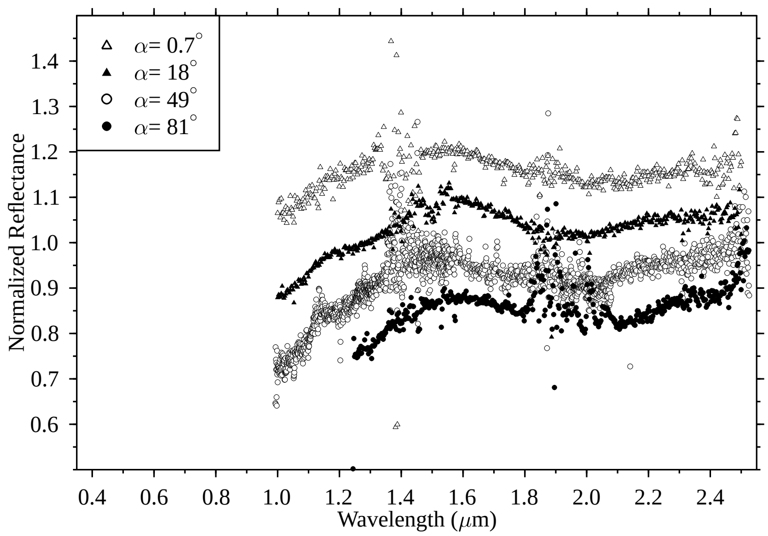

Figure 2: 4179 Toutatis observed on 4 dates with phase angles from 1-80 degrees. From bottom 2000 December 01, 81 degrees; 2000 December 22, 49 degrees; 2001 January 14, 18 degrees; 2001 February 01, 0.7 degrees. Each spectrum has been offset vertically by 0.1 for clarity.

Nonetheless, if we then assume that any phase reddening is negligible we can invert the experiment and use the data to search for variations in surface compostion with rotational phase. For many NEOs, which have rotation periods of a few hours, the relatively long period required to obtain CGS4 spectra (usually about 3 hours) would make rotational phase resolved spectroscopy impossible. However 4179 Toutatis has a rotation period of almost 130 hours, so a typical CGS4 observing session represents a small fraction of a rotation. Thus if large surface inhomegenities were present there is a good chance that our 4 independent spectra would detect them. However examination of Fig.2 shows that all four spectra are indistiguishable and this rules out such spectral diversity. This result also provides (on the assumption of no phase reddening) a further consistency check of our spectral splicing technique since data on four nights, with two different ratio stars, produce indistiguishable results.

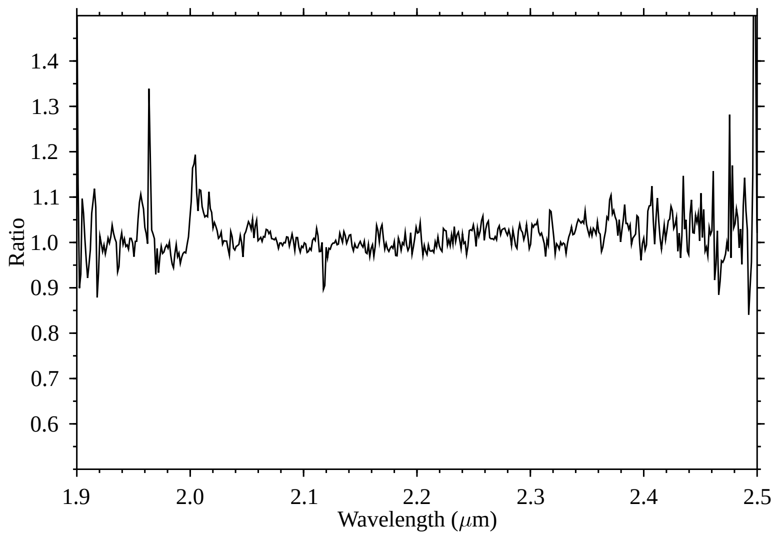

Figure 3: Ratio of K band reflectances of 4179 Toutatis on 2000 December 01 and 2001 February 01. There is no evidence for any systematic reddening despite the change in phase angle by 80 degrees.

6.3 5381 Sekhmet

This object is a radar observed binary asteroid with a primary having an estimated diameter of 1km and a secondary of about 300m. No taxonomic class has been published. It was observed twice by us in May 2003 using the UIST spectrometer. Observations on 2003 Sep 05 produced the high signal to noise spectrum between 1.4–2.5μm shown in Fig.4. A further observation was made on 2003 September 07 under less favourable observing conditions (scattered clouds and a relatively high water vapour column). Although of lower signal to noise, and suffering from poorer cancelation of the atmospheric features between 1.8–1.9μm, this spectrum is indistinguishable in shape from that shown and is not repeated here.

Delbo (2004) gives a diameter of 1.3–1.5 km, and p_v = 0.22–0.28 from thermal-IR observations, assuming H = 16.5. The deep pyroxene absorption band around 1.9μm (Fig. 4) is suggestive of a V-type spectral classification, which would be compatible with Delbo's albedo value. This suggested classification is supported by an unpublished optical spectrum provided to us by E. Howell which shows an absorption at 0.95μm and a further absorption around 0.65μm.

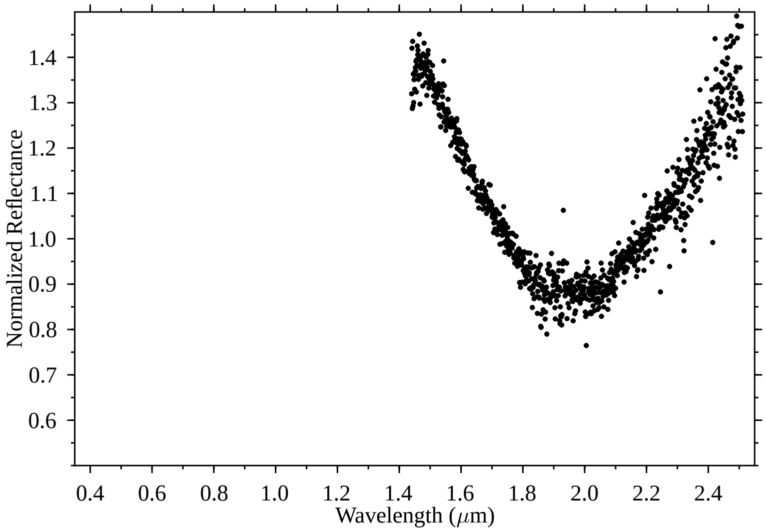

Figure 4: 5381 Sekmet observed with UIST on 2003 May 05. Data from the region of poor transmission shortward of 1.45μm and a few clearly anomalous points have been manually removed from the data before plotting.

6.4 (5587) 1990SB

This object provides an excellent possibility for data comparison having been observed by us on 2001 March 31 and on two different occasions by Binzel et al (2004). Our spectrum was compiled from 5 grating settings covering the range 0.8-2.5μm. The spectrum of Binzel et al (2004) covers 0.55–1.0μm and further as yet unpublished spectrum supplied to us by R.P Binzel covers the range 0.5–2.5μm.

Fundamentally the three datsets are similar, but there are inconsistencies in the depth and shape of the features between both the two spectra of Binzel et al (2004), and between our spectrum and those of Binzel. The main difference between our spectrum and those of Binzel arises at the point where the spectra span the region of poor transmission around 1.4μm (ie between the J and H windows). Our data were taken under dry conditions with airmass matches between the asteroid and ratio star always better then 0.1 airmasses, so atmospheric cancellation should have been excellent.

The spectral type of this Amor asteroid is Sq, according to the taxonomic classification of Bus and Binzel (2002). Delbo et al. (2003) derived a diameter of 3.6 $\pm$ 0.6 km and p_v = 0.32 $\pm$0.1. The Sq spectral type and albedo are both consistent with the deep absorption features around 0.9μm and 1.9μm evident in the UKIRT spectrum (Fig.5).

6.5 6489 Golevka

We obtained observations of this object during two apparitions, between 1.1-2.4μm on 1999 May 19 and 1999 June 6 with CGS4 and between 1.4–2.5μm on 2003 May 11 with UIST. The data on 1999 May 28 cover the range 1.2–2.4μm, that on 1999 June 6 was a single grating covering 1.9–2.5μm. Agreement between these data are excellent and so we have merged the

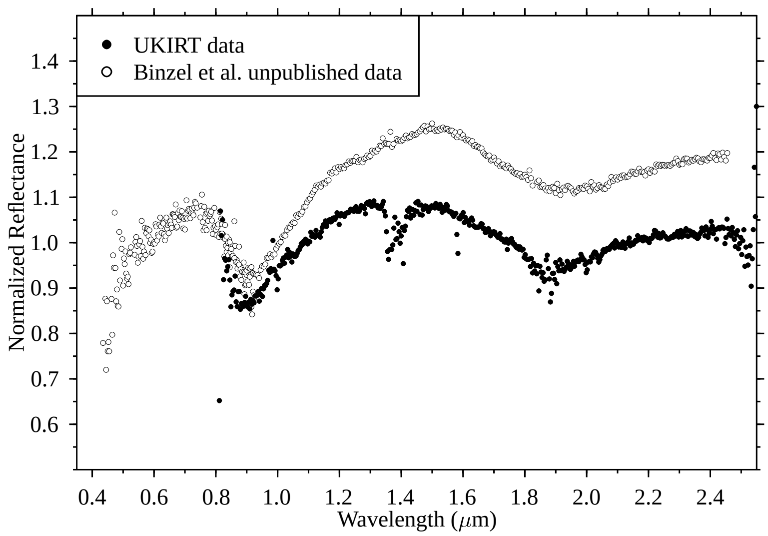

Figure 5: (5587) 1990 SB. UKIRT data and unpublished data by Binzel at al. Note that the Binzel spectrum has not been renormalised to 2.2μm and so has a vertical shift relative to the UKIRT spectrum below. The 'feature' at around 1.35μm in the UKIRT spectrum is an artifact of poor atmospheric cancellation.

two datasets to produce a composite spectrum. There are also data published by Binzel et al (2004) between 0.5 and 1.6μm.

The UIST spectrum between 1.4–2.5μm taken on 2003 May 11 has comparable signal to noise as our 1999 data. This is taken through a single grism and fits well with our 1999 H and K CGS4 data, giving further confidence in reliability of our spectral fragment splicing process.

Finally, having satisified ourselves of the quality of the CGS4 data, we combined this with observations from Binzel et al (2004) to produce the composite spectrum shown in Fig.6.

From an extensive set of radar observations Hudson et al. (2000a) derived an equivalent spherical diameter for this very irregular Apollo asteroid of 0.53 $\pm$ 0.03 km. Taking H = 19.07 $\pm$ 0.03 from Mottola et al. (1997), this diameter implies p_v = 0.15 $\pm$ 0.02. Hudson et al. (2000a) conclude that the radar scattering properties and previously published optical scattering properties are consistent with those of a typical S-class asteroid. However, Bus and Binzel (2002) classify Golevka as Q-type. The similarity of the combined spectrum of Golevka (Fig.6) with those of Sq-types 5587 (Fig. 5), and 11405 (Fig. 7) is evident (see also 52760 and 66391, Figs. 12, 13).

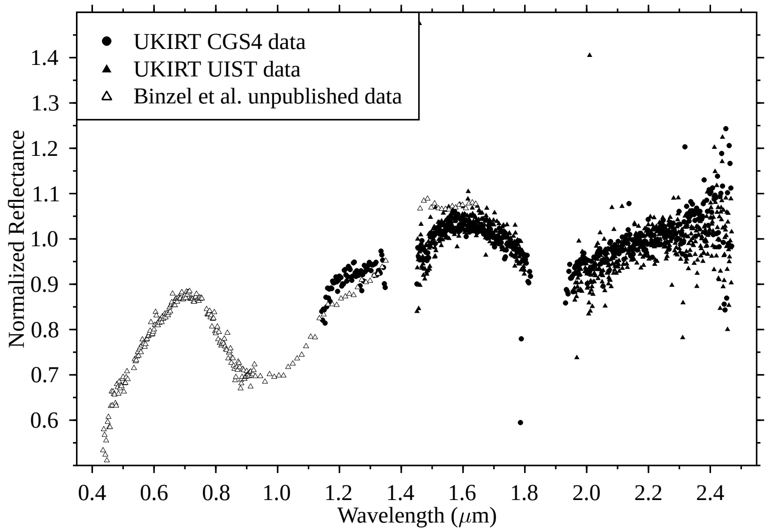

Figure 6: 6489 Golevka. UKIRT data of 1999 and 2003 with data of Binzel et al (2004) overplotted. Excessively noisy data at the overlaps of the J_L/H and H/K windows have been removed.

6.6 (11405) 1999 CV_3

This Apollo object was observed on 1999 February 19 using three grating settings covering 1.2–2.5μm. Our data match those of Binzel et al (2004) well, allowing us to produce a good quality composite spectrum from 0.5–2.5μm (Fig.7).

The asteroid has been classified as Sq by Binzel et al. (2004). The spectral type is identical to that of (5587) 1990 SB (cf. Fig.5), although the broader 0.9μm absorption in the case of (11405) 1999 CV_3 may indicate a more significant presence of olivine. No further measurements of physical properties of this object appear to have been made to date.

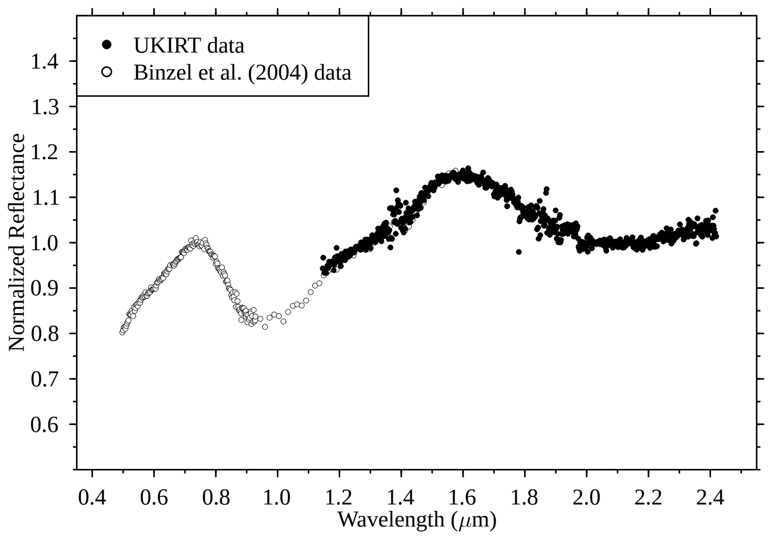

Figure 7: (11405) 1999 CV_3 UKIRT data plus data of Binzel et al (2004).

6.7 (14402) 1991 DB

This object was observed on 2000 March 12. Our spectrum extends from 0.99 to 2.52μm and was taken using four grating settings. Although fairly flat between 1.6 and 2.5μm the spectrum slopes away shortward of 1.6μm and is still falling when the spectrum ends. Comparison of our spectrum with that of Binzel (Fig.8) shows that his spectrum shows a much shallower absorption feature around 1μm. We have examined our data and do not detect any anomalies in it. Spurious slopes might arise due to poor atmospheric cancellation, but in the short wavelength observations which make up the composite spectrum the airmass match from asteroid to ratio star was good (better than 0.1 airmass). Furthermore there is no evidence of excess noise in the regions of low atmospheric transmission (eg around 1.4 and 1.8μm) which might also be expected if atmospheric cancellation problems existed. Finally the slope does not occur in just a single spectral fragment but is manifest in both the J_{long} and J_{short} sub spectra.

This Amor asteroid has been classified as C-type by Binzel et al. (2004). However, the differences between the UKIRT spectrum and that from Binzel et al. (2004) are puzzling.

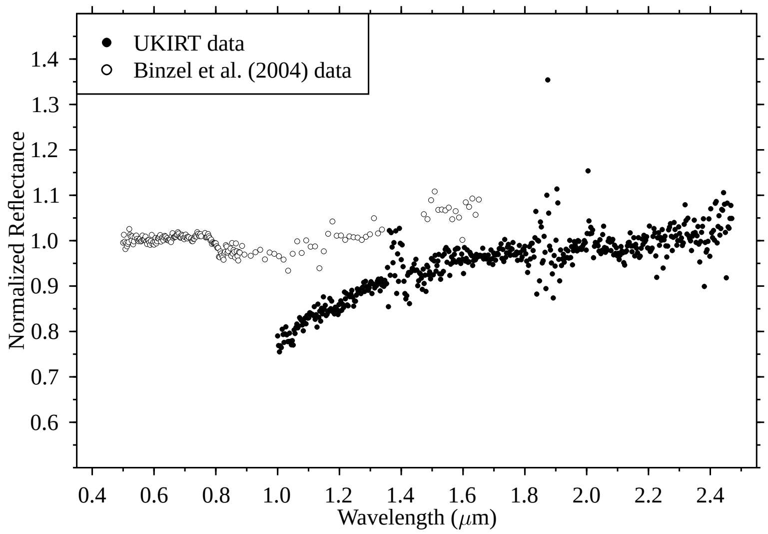

Figure 8: (14402) 1991 DB UKIRT data and data from Binzel et al (2004).

The C taxonomic class is characterized by a relatively flat, featureless spectrum from 0.5–2.5μm. The UKIRT data reveal a significant positive slope, steeper than that normally associated with C-type asteroids. For example, compare the UKIRT spectrum in Fig.8 with the C-type spectra of (25330) 1999 KV_4 (Fig. 11), 2100 Ra-Shalom, 1998 HT_{31}, 1998 KU_2 (Binzel et al. (2004). Furthermore, Delbo et al. (2003) derived $p_v = 0.14 \pm 0.02$ (and diameter $= 0.6 \pm 0.09$ km, taking $H = 18.85 \pm 0.1$) for this object from thermal-IR observations, which is significantly higher than normal for C-type asteroids. Alternative classifications consistent with a red featureless spectrum are M and E. The moderate albedo of 0.14 rules out E type, which is normally associated with very high albedos of 0.3 or more, but is in the normal range for M-type asteroids.

On the basis of the above discussion and the similarity between the UKIRT spectrum and that of the M-type main-belt asteroid 16 Psyche (see Gaffey et al. 1989), we suggest an M-type classification for (14402) 1991 DB.

6.8 25143 Itokawa

Asteroid 25143 Itokawa was the objective of the JAXA Hayabusa rendezvous and sample return mission. The spacecraft successfully entered orbit around the asteroid in 2005, although subsequent technical problems make it unclear if any samples will ever be returned to Earth. An extensive observing campaign was undertaken during the asteroid's close approach to Earth in 2001 in preparation for the mission and 25143 Itokawa has been well characterised. A 0.5 to 2.5μm spectrum was obtained by Binzel et al. (2001) which revealed a red-sloped S(IV) type spectrum with strong 1 and 2 μm absorption bands. These features indicate an ordinary chondrite composition with a spectrum reddened by space weathering. The Hayabusa spacecraft payload included a near infrared spectrometer which has taken 80,000 spectra of spatially resolved regions on the asteroid between 0.76 and 2.1μm. Preliminary results have been presented by Abe et al. (2006) which showed broad agreement with the disk-integrated data, but showed albedo, band depth and spectral slope variations with position on the nucleus.

25143 Itokawa was observed twice in all five wavelength ranges of CGS4 on each of 17 and 18 March 2001. Each fragment was reduced individually using the ratio star BS5364. The derived fluxes in each fragment showed evidence of the light curve (amplitude approx 0.75 mag) but only marginal evidence for any color changes with rotation (Fig.9).

Since each sub-spectrum was taken at a different rotational phase, it was not possible to produce a composite spectrum for a fixed rotational phase. The data from the four separate reflection spectra in each wavelength fragment were therefore combined to improve the signal to noise ratio near the edges of the window and to average out any small rotational effects if present. This was achieved by removing the noisy data at the edges of the window where transmission was negligible and then taking the average of the 4 fragments, after normalising

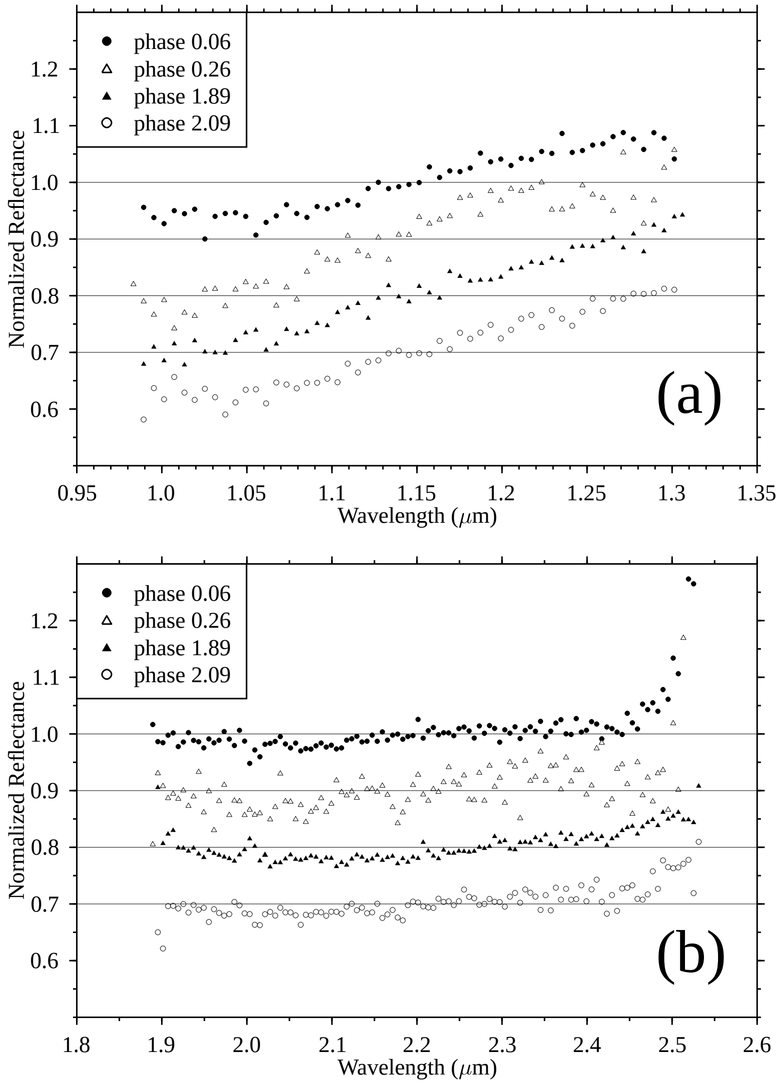

Figure 9: Relative reflectance for the four spectra in each of two spectral fragments. Apart from the upper spectrum in a), there is no evidence for spectral variations with rotational phase. a) J_{short} band: solid circles taken at rotational phase of 0.06 (where phase = 0 corresponds to the time of the first spectrum on 17 March and the rotation period is 12.118 hours derived from the J-band photometry and unpublished optical photometry); open squares at rotational phase of 0.26, and reflectance offset by -0.1; solid squares at rotational phase of 1.89, and reflectance offset by -0.2; open circles at rotational phase of 2.09, and reflectance offset by -0.3. b) K band: solid circles taken at rotational phase of 0.17 open squares at rotational phase of 0.35, and reflectance offset by -0.1; solid squares at rotational phase of 2.02, and reflectance offset by -0.2; open circles at rotational phase of 2.20, and reflectance offset by -0.3.

each fragment over the central region where the data had a high signal to noise ratio. The data were then binned to a resolution of 0.006μm. The splicing of the sub-spectra to produce a single spectrum was performed using only high signal to noise data in the overlap regions of each fragment. The result, normalised to unity in the K window, is shown in Fig.10a.

For 25143 Itokawa we also obtained infrared photometry and a light curve in the same period as the spectroscopy. This allows a direct comparison between spectra spliced section by section and the relative reflectance derived using photometry corrected for any light curve variations.

Broadband JHK photometry was obtained at UKIRT using the infrared camera IRCAM on 19 March 2001 when conditions were photometric. The camera is equipped with a 256 x 256 InSb array, with a plate scale of 0.286 arcsec per pixel, giving a field of view of 73.2 arcsec. Images were taken through the standard J, H and K infrared filters (with mean wavelengths of 1.25, 1.65 and 2.2μm) in sequences such as JHJKJ. The observations were made and reduced using standard jittering techniques to obtain a median filtered flat-field from the science frames as described in Davies et al. (1998).

Instrumental magnitudes were extracted using 5 arcsec apertures. Instrumental J magnitudes were interpolated to the time of the other filters to account for light curve variations. Instrumental colors were then determined and calibration was performed using UKIRT standard FS135. The derived mean colors are J-H = 0.46$\pm$ 0.02 and J-K = 0.51$\pm$0.02. The uncertainties are dominated by calibration uncertainties. These results are consistent with the photometry of Ishiguro et al. (2003) who found J-H = 0.49$\pm$0.04 and H-K = 0.02$\pm$0.04.

The relative reflectance values (normalised at a wavelength of 2.2 μm) were obtained from:

$$R = 10^{0.4[(m_K - m_X) - (m_K - m_X)_O]}$$

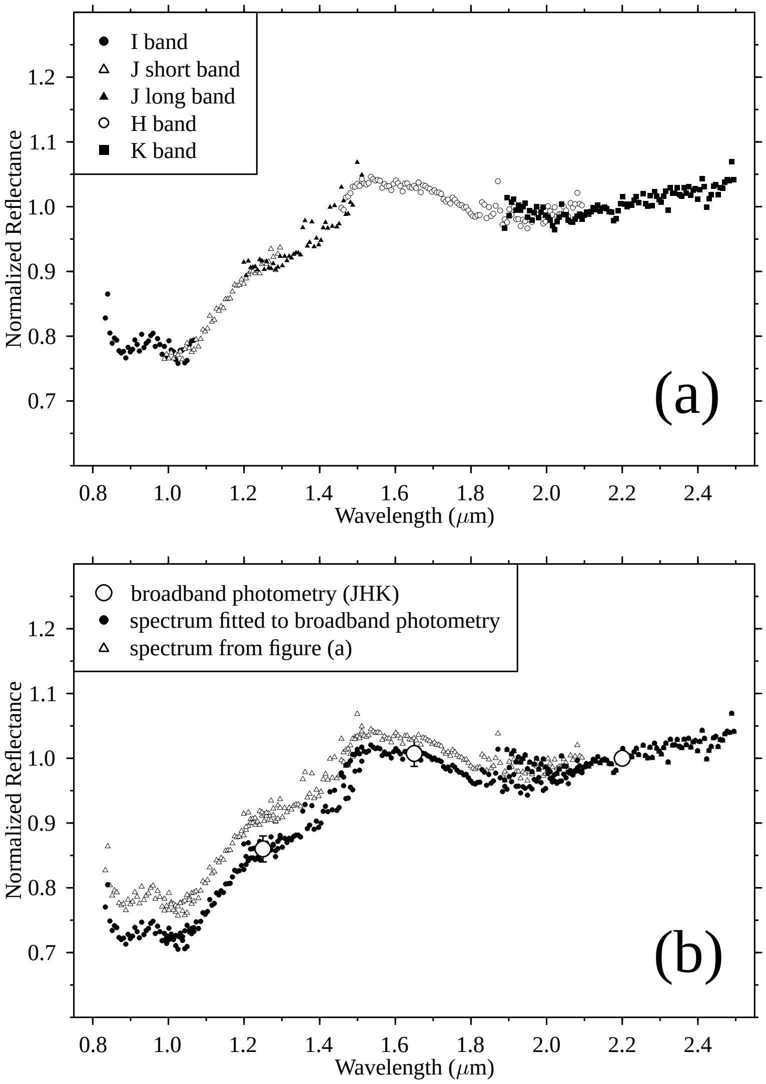

Figure 10: a) Reflectance spectrum of 25143 Itokawa produced by fitting overlap regions of spectral fragments, normalised to the K band spectrum between 2.15 and 2.25μm. b) Comparison of reflectance spectrum of 25143 Itokawa produced by fitting overlap regions of spectral fragments from Fig. 10a (open triangles) to that produced by fitting spectral fragments to broadband photometry (solid circles).

where $(m_K - m_X)_O$ is the solar color for filter passband X. Solar colors of J-K = 0.35 and H-K = 0.06 (Degewij et al., 1980) gave relative reflectance at J of R_J=0.86±0.02 and at H of R_H = 1.01±0.02.

Fig. 10b shows the spectral fragments fitted to the relative reflectance derived from the photometry (except for the I band data). The photometry-fitted data are somewhat redder than the spliced data and essentially in agreement with the spectrum of Binzel et al. (2001). We therefore confirm the Binzel et al classification. This comparison indicates that the splicing technique can cause small spurious spectral slopes across the entire waveband which may introduce errors in any band depth derivations. However, the small and large scale spectral features are still identifiable and a qualitative classification is possible from spliced data.

6.9 (25330) 1999 KV_4

Our spectrum was taken on 2003 May 6 with the UIST instrument and so no spectral splicing was necessary. The object was also observed by Lazzarin et al (2004) but unfortunately this dataset cuts off at 1.35μm whereas ours does not cut on until 1.45μm. Therefore a direct merging is not possible. We have arbitralily normalised our spectrum to an extrapolated value of the Lazarrin data at 1.6μm and both spectra are plotted together in Fig.11.

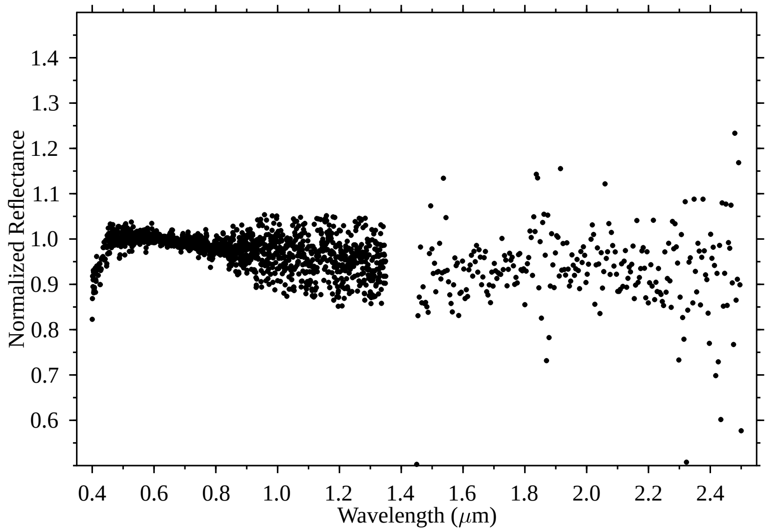

Figure 11: (25330) 1999 KV_4.

The spectrum of this Apollo asteroid is essentially flat throughout the 0.5–2.5μm range, consistent with both the C classification of Lazarin et al. (2004) and the B classification of Binzel et al. (2004). Furthermore, Delbo (2004) gives $p_v = 0.05$–0.09 (and diameter = 2.5–3.2km, taking H = 16.3) for this object from thermal-IR observations, which is compatible with both C and B spectral types.

6.10 (52760) 1998ML$_{14}$

This object presented an observational challenge, being a morning object becoming accessible to the UKIRT telescope at its airmass limit of 2 only a few minutes before twilight. Since there was insufficient time to obtain more than two grating settings before the sky brightened, the data were taken over the three dates 1998 August 11, 12 and 13 using 1, 2 and 2 grating settings respectively. In order to effectively match airmasses with the ratio star, critical at these high airmasses, two different ratio stars were used on each of the 2nd and 3rd nights. This was necessary because no single ratio star was sufficiently close to the asteroid that it would remain at a matching airmass for long enough to make two observations in different grating settings. All five datesets were then combined to make the composite spectrum which runs from 1.2–2.5μm. Atmospheric cancellation is excellent considering the high airmass of the observations.

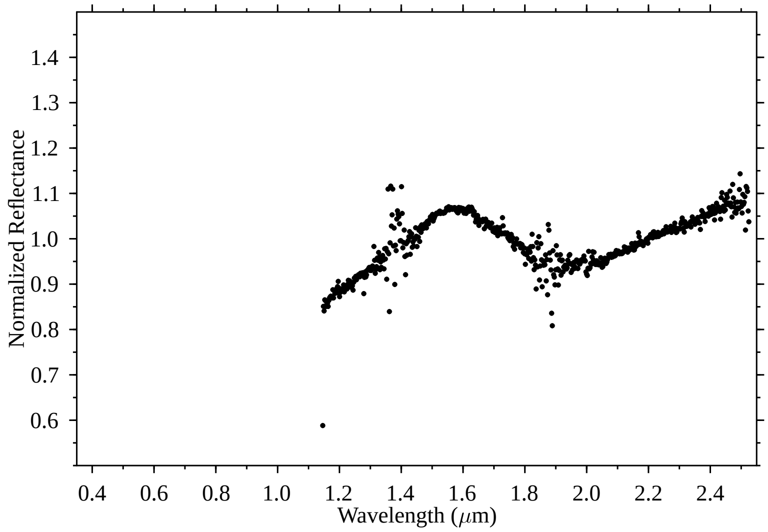

Figure 12: (52760) 1999 ML$_{14}$.

Ostro et al. (2001) conclude on the basis of radar and optical observations that this object is roughly spheroidal with a diameter of about 1 km, $p_v = 0.17$, and radar and optical properties typical of S-type asteroids. The UKIRT spectrum (Fig. 12) displays significant pyroxene absorption around 1.9 μm, which is consistent with an S or Sq classification (cf. Figs. 5, 6, 7, 13). The lack of spectral data at shorter wavelengths precludes any further discussion of spectral type.

6.11 (66391) 1999 KW_4

This asteroid is a Mercury-crossing Aten and a potentially hazardous object that approached the Earth at a minimum distance of 0.032 AU on 2001 May 25; it was observed on 2001 May 21-23 with the Goldstone radar antenna (Benner et al., 2001). The resulting delay-Doppler images not only revealed the presence of a moon but also resolved its orbital motion around the primary body. The diameter of the primary is around 1.2 km and that of the moon around 0.4 km.

Our observations were made on 20 May 2001, a particularly favourable apparition making it possible to cover all 5 grating settings and obtain a spectrum from 0.8–2.5μm. This is in good agreement with data of Binzel et al (2004) covering the range 0.9–1.5μm and further confirms the validity of our spectral splicing method. The resulting spectrum of (66391) 1999 KW_4 is shown in Fig. 13.

The origin of binary systems in the NEO population is a subject of lively debate, and one of considerable significance given that up to 20 percent of the NEO population may be binary (Pravec et al., 2006). In the case of (66391) 1999 KW_4 the steeply inclined (i = 38.9 deg.) "comet-like" orbit led to speculation that this binary system may be the result of the break up of a cometary nucleus. However, the deep absorption bands of olivine and pyroxene evident in the CGS4 spectrum around 0.95μm and 2.0μm strongly suggest that this object is a stony asteroid of class S or similar, which is consistent with the albedo (p_v of approximately 0.3) implied by the radar diameter. An alternative model of binary system

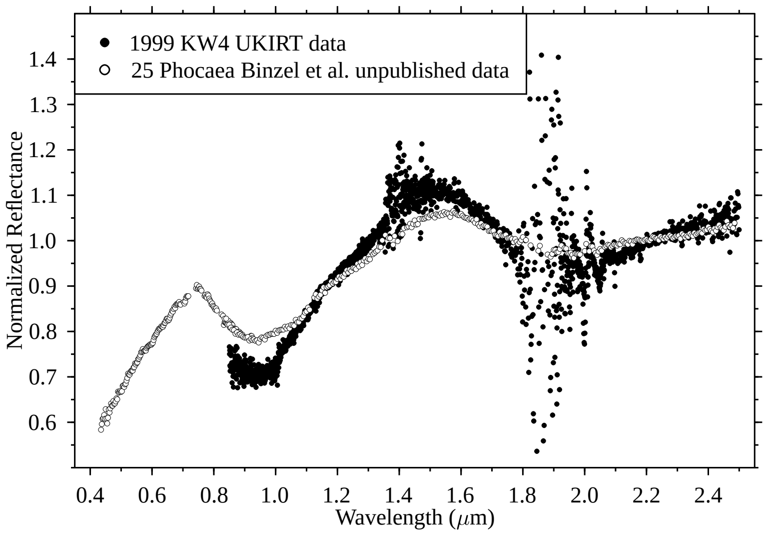

Figure 13: (66391) 1999 KW_4 compared with the main belt object 25 Phocaea.

formation, such as the tidal disruption of a rubble pile during a close approach to a planet, may be applicable in the case of (66391) 1999 KW_4

The S class has been subdivided into subclasses by Gaffey et al. (1993), with the subclasses distinguished from one another by differing ratios of the areas of the 1- and 2-μm absorption bands. The 1999 KW_4 spectrum is of high-enough quality to allow these determinations to be made, but the wavelength coverage does not allow the 1-μm band area to be measured. We have compared the spectrum to that of 25 Phocaea and find that it is similar but with stronger bands, suggesting that it has suffered less 'space weathering' than the larger main belt object. Therefore we suggest that 1999 KW_4 could be classed as an S(IV) object.

6.12 (101955) $1999RQ_{36}$

This Apollo object was observed on 22 September 1999 in the H and K windows. Airmass matches with the ratio star were excellent, better than 0.04 airmass, and both observations were made close to zenith (AM = 1.2 and 1.03). On 23 September 1999 two J spectra were taken, both close to zenith (AM= 1.07, 1.08) and with the ratio star matched to 0.02 airmass or better.

The apparent emission feature between 1.3 and 1.5μm is an artifact of poor atmospheric cancellation in the J_{long} window, which is surprising due to the good airmass match.

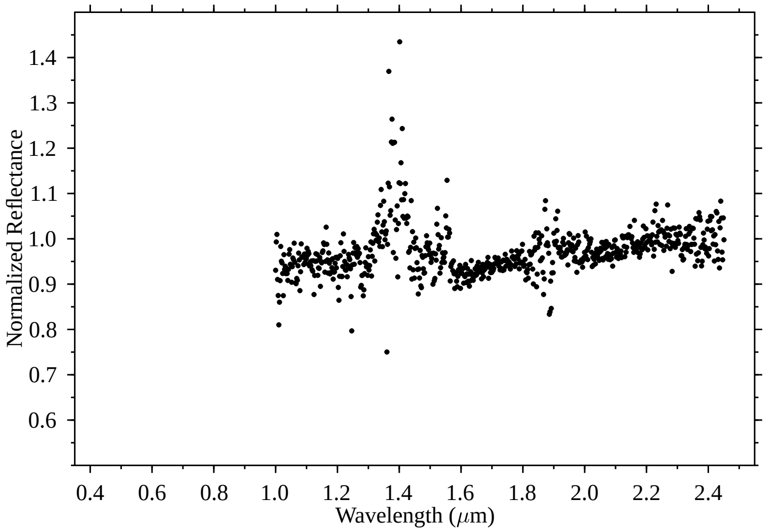

Figure 14: (101955) $1999RQ_{36}$.

Hudson et al. (2000b) report a size of about 500m and a surprisingly spherical shape from radar observations. This size implies p_v of about 0.036, assuming H = 20.72 (Krugly et al., 2002). The UKIRT spectrum (Fig.14) shows no sign of absorption features and is thus indicative of a C, M, or E classification, or similar. The low albedo would rule out M and E, thus this object appears to have a very dark, carbonaceous surface. Lack of optical observations precludes further discussion of taxonomic type.

7 Summary

For a complete understanding of the physical properties of near-Earth asteroids it is necessary to combine data obtained from all relevant observing techniques and spectral regions. Optical and infrared photometry can constrain parameters such as rotation vectors, shapes, sizes, and albedos and provide clues to taxonomic type; radar observations can provide information on shapes and surface properties, including composition. However, detailed knowledge of the diverse mineralogy of asteroids can be gained only via spectroscopy. Asteroid taxonomy is traditionally based on optical spectroscopy but, as our results confirm, the near-infrared region provides important additional information, which is necessary for a complete picture of asteroid mineralogy.

We have discussed the problems associated with merging asteroid spectral data taken with different instruments and/or at different times. The production of composite spectra is fraught with difficulties, such as lack of adequate overlap, poor signal-to-noise ratio at the extremities of an instrument's spectral range, rotational variability of the target, and variability of observing conditions. We have taken great care to minimize the errors arising from merging spectral fragments and have verified our techniques by comparison with similar spectra taken in our programme at different times and with data available in the literature. We are confident that our spectral merging techniques are not giving rise to systematic distortions in overall spectral shape.

We have presented spectral data for 12 near-Earth asteroids with diverse properties and compared our results with information on individual objects available in the literature.

Two of the objects observed, (25330) 1999 KV_4, and (101955) 1999 RQ_{36}, have relatively flat, featureless spectra and dark surfaces with albedos below 0.1, suggestive of carbonaceous compositions. In the case of 25330 our results are consistent with the C and B classifications of other authors.

Our spectrum for (14402) 1991 DB is featureless but has a significant positive slope in the range 1 – 2.5 μm. The moderate albedo of 0.14 $\pm$ 0.02 (Delbo et al., 2003) is higher than that normally associated with B, C spectral types, but well below that associated with E types, which also exhibit featureless spectra. We conclude that the available data suggest that 14402 belongs to the relatively rare M class. The nine remaining asteroids in our sample exhibit spectra consistent with S, Q, or V taxonomic types.

In the cases of 5381 Sekhmet and (52760) 1998 ML_{14} no taxonomic classes appear to have been published to date. The deep pyroxene absorption band around 1.9 μm seen in our UKIRT spectrum of 5381 Sekhmet is suggestive of a V-type classification. The significant but less pronounced 1.9 μm absorption seen in our spectrum of 52760 is consistent with S or Sq type.

For all other objects in our programme the UKIRT spectra are consistent with published spectral classifications.

Asteroid	Deduced Spectral Type	Asteroid	Deduced Spectral Type
1627 Ivar	S	14402 1991 DB	M
4179 Toutatis	S	25143 Itokawa	S(IV)
5381 Sekhmet	V	25330 1999 KV_4	C or B
5587 1990 SB	Sq	52760 1998 ML_{14}	S or Sq
6489 Golevka	Sq	66391 1999 KW_4	S(IV)
11405 1999 CV_3	Sq	101955 1999 RQ_{46}	C

Table 3: Summary of Spectral Types.

Four spectra of 4179 Toutatis taken over a very wide range of solar phase angle (0.7deg - 81deg) and at intervals of several weeks are indistinguishable within the uncertainties and therefore do not reveal any evidence for phase reddening or surface variegation.

8 Acknowledgements

We thank all the technical staff of UKIRT for its support of these observations and in particular we acknowledge the long suffering Telescope System Specialists (Thor Wold and Tim Carroll) for their help in aquiring these often faint, always moving, targets. T. R. Geballe obtained the data on (101955) 1999RQ$_{36}$ on our behalf. A.S. Rivkin acknowledges NASA Planetary Geology and Geophysics grant NNG06GA23G. We thank R.P. Binzel for permission to use his unpublished spectra and the helpful input from the two reviewers on the original manuscript.

UKIRT is operated by the Joint Astronomy Centre on behalf of the UK Particle Physics and Astronomy Research Council.

9 References

Abe, M., Takagi, Y., Kitazato, K., Hiroi, T., Abe, S., Vilas, F., Clark, B.E., Abell, P.A., Lederer, S.M., Jarvis, K.S.,Nimura, T., Ueda, Y., Fujiwara, A. (2006) Preliminary Results from the Hayabusa Near Infrared Spectrometer (NIRS) of Asteroid (25143) Itokawa, Lunar. Planet. Sci. Conf. 37, abstract no.1547.

Binzel, R.P., Rivkin, A.S., Bus, S.J., Sunshine, J.M., Burbine, T.H., (2001) MUSES-C target asteroid (25143) 1998 SF36: A reddened ordinary chondrite. Meteoritics & Planet. Sci. 36, 1167-1172.

Binzel, R.P., Rivkin, A.S., Stuart, J.S., Harris, A.W. Bus, S.J. and Burbine, T.H. (2004) Observed Spectral Properties of Near Earth Objects: Results for Population Distribution, Source Regions and Space Weathering Processes. Icarus 170 pp 259–294

Benner, L.A.M., Ostro, S.J., Giorgini, J.D., Jurgens, R.F., Margot, J.L., Nolan, M.C., (2001). 1999 KW4. IAU Circ., 7632.

Bus, S.J. and Binzel, R.P. (2002) Phase II of the Small Main-Belt Asteroid Spectroscopic Survey, A Feature-Based Taxonomy. Icarus, 158, 146-177

Davies, J.K., McBride, N., Ellison, S.L., Green, S.F., Ballantyne, D.R., (1998) Visible and Infrared Photometry of six Centaurs. Icarus, 134, 213-227.

Degewij, J., Cruikshank, D.P., Hartmann, W.K., (1980) Near-infrared colorimetry of J6 Himalia and S9 Phoebe - A summary of 0.3- to 2.2-micron reflectances. Icarus, 44, 541-547.

Delbo, M., (2004). The nature of near-Earth asteroids from the study of their thermal infrared emission. PhD thesis. Freie Universitt, Berlin.

Delbo, M., Harris, A. W.,Binzel, R.P., Pravec, P. and Davies, J.K., (2003) Keck Observations of Near-Earth Asteroids in the Thermal Infrared. ICARUS 166, 116-130

Gaffey, M.J., Bell, J.F., Cruikshank, D.P., (1989). Reflectance spectroscopy and asteroid surface mineralogy. In: Binzel, R. P., Gehrels, T., Matthews, M. S. (Eds.), Asteroids II. Univ. of Arizona Press, Tucson, pp. 98-127.

Gaffey, M.J., Burbine, T.H., Piatek, J.L., Reed, K.L., Chaky, D.A., Bell, J.F., Brown, R. H. (1993) Mineralogical variations within the S-type asteroid class. ICARUS 106, 573-602

Howell, E.S., Britt, D.T., Bell, J.F. Binzel R.P., and Lebovsky, L. (1994) Visible and Near-

Infrared Spectral Observations of 4179 Toutatis. Icarus 111 468-474.

Hudson, R.S., Ostro, S.J., Jurgens, R.F., Rosema, K.D., Giorgini, J.D., Winkler, R., Rose, R., Choate, D., Cormier, R.A., Franck, C.R., and 17 coauthors (2000a) Radar Observations and Physical Model of Asteroid 6489 Golevka. Icarus 148, 37-51

Hudson, R.S., Ostro, S.J., Benner, L.A.M., (2000b). Recent Delay-Doppler Radar Asteroid Modeling Results: 1999 RQ_{36} and Craters on Toutatis. Bull. Am. Astron. Soc. 32, 1001.

Ishiguro, M., Abe, M., Ohba, Y.,Fujikawa, A., Fuse, T.,Terada, H., Goto, M., Kobayashi, N., Tokunaga, A.T., Hasegawa, S. (2003) Near-infrared observations of MUSES-C mission target. Publ. Astron, Soc, Japan, 55, 691-699.

Kiselev, N.N., Chernova,G.P., and Lupisko, D.F. (1994) Polarimetry of asteroids 1036 Ganymed and 1627 Kinemat. Fis. Nebesn. Tel., vol. 10, 35-39

Krugly, Yu.N., Belskaya, I.N., Shevchenko, V.G., Chiorny, V.G., Velichko, F.P., Mottola,S., Erikson, A., Hahn, G., Nathues, A., Neukum, G., Gaftonyuk, N.M., Dotto E., 2002. The near-Earth objects follow-up program IV. CCD photometry in 1996-1999. Icarus 158, 294-304.

Lazzarin, M., Marchi, S., Barucci, M.A. Di Martino, M. and Barbieri, C. (2004) Visible and Near Infrared Spectroscopic Investigations of Near-Earth Objects at ESO: First Results. Icarus 169, 373-384.

Luu, J.X. and Jewitt, D.C. (1990). Charge Coupled Device Observations of Asteroids: I Near-Earth and 3:1 Resonance Asteroids. Astronomical Journal 99,(6) 1985–2011

Mottola, S. et al (1997) "Physical Model of Near-Earth Asteroid 6489 Golevka (1991JX) from Optical and Infrared Observations." Astron J. 114 (3) 1234-1245.

Ostro, S.J., Campbell, D.B., Hine, A.A., Shapiro, I.I., Chandler, J. F., Werner, C.L., Rosema, K.D.(1990) Radar images of asteroid 1627 Ivar. Astron J. 99, 2012-2018, 2072.

Ostro, S.J., Hudson, R.S., Benner, L.A.M., Nolan, M.C., Giorgini, J.D., Scheeres, D.J., Jurgens, R., Raymond, F., Rose, R.(2001) Radar observations of asteroid 1998 ML_{14}. Meteoritics and Planetary Science, 36, (9) 1225-1236

Pravec, P. and 56 colleagues, 2006. Photometric survey of binary near-Earth Asteroids. Icarus, 181, (1) 63-93

10 Tables: Repeated

Setting Label	Central wavelength of window (μm)	CGS4 Min (μm)	CGS4 Max (μm)	Comment
K	2.2	1.88	2.52	Includes long end of H window.
H	1.65	1.44	2.08	Includes overlap with K and J_{long}
J_{long}	1.25	1.24	1.56	
J_{short}	1.25	0.99	1.31	Limited overlap with J_{long}.
I	0.9	0.78	1.1	Rarely used.

Table 4: Table 1. Typical CGS4 spectral ranges used.

Target Name	Date	R (AU)	δ (AU)	Phase Angle (deg)	V Mag	Lambda Range (μm)	No of Grating Settings	Ratio Star
1627 Ivar	2000 Mar 12	2.075	1.089	4.92	15.2	1.25–2.5	3	BS4437
4179 Toutatis	2000 Dec 01	0.997	0.187	81.0	14.6	1.2–2.5	3	BS4437
4179 Toutatis	2000 Dec 22	1.138	0.269	49.1	14.7	1.0–2.5	4	BS4437
4179 Toutatis	2001 Jan 14	1.329	0.372	18.6	14.8	1.0–2.5	4	BS3510
4179 Toutatis	2001 Feb 01	1.487	0.502	0.7	14.8	1.0–2.5	4	BS3510
5381 Sekhmet	2003 May 05	1.087	0.206	62.4	15.5	1.4-2.5	1	BS7260
5381 Sekhmet	2003 May 07	1.095	0.186	58.0	15.1	1.4-2.5	1	BS7260
5587 1990 SB	2001 Mar 31	1.465	0.518	21.0	14.0	0.80–2.5	5	BS5384
6489 Golevka	1999 May 19	1.053	0.051	38.6	14.4	1.14–2.42	3	BS6060
6489 Golevka	1999 Jun 8	1.029	0.059	74.5	15.7	1.9–2.5	1	BS8314
6489 Golevka	2003 May 11	1.103	0.113	33.0	16.1	1.4–2.5	1	16 Cyg B
11405 1999 CV_3	1999 Feb 19	1.216	0.236	14.5	13.1	1.15–2.4	3	BS402
14402 1991 DB	2000 Mar 12	1.089	0.107	26.1	14.9	0.99–2.52	4	BS4437
25143 Itokawa	2001 Mar 17	1.049	0.064	31.4	14.7	0.8–2.5	5	BS5364
25143 Itokawa	2001 Mar 18	1.046	0.061	33.2	14.6	0.8–2.5	5	BS5364
25143 Itokawa	2001 Mar 19	1.042	0.058	35.2	14.5	JHK		Photometry
25330 1999 KV_4	2003 May 06	1.251	0.351	11.0	15.5	1.4–2.5	1	BS5657
25330 1999 KV_4	2003 May 09	1.368	0.362	7.42	15.5	1.4–2.5	1	BS5657
52760 1998 ML_{14}	1998 Aug 11	1.013	0.02	91.4	12.3	1.88–2.5	1	BS1747
52760 1998 ML_{14}	1998 Aug 12	1.008	0.02	104.2	13.2	1.4–2.0	1	BS153
52760 1998 ML_{14}	1998 Aug 12	1.008	0.02	104.2	13.2	1.9–2.5	1	BS1747
52760 1998 ML_{14}	1998 Aug 13	1.002	0.02	113.9	14.1	1.14–1.45	1	BS1532
52760 1998 ML_{14}	1998 Aug 13	1.002	0.02	113.9	14.1	1.64–2.26	1	BS1747
66391 1999 KW_4	2001 May 29	1.051	0.053	43.7	11.8	0.8–2.5	5	BS5534
101955 1999 RQ_{46}	1999 Sep 22	1.004	0.015	86.7	14.7	1.43–2.52	2	BS220
101955 1999 RQ_{46}	1999 Sep 22	1.001	0.014	97.8	15.3	1.0–1.55	2	BS2208

Table 5: Table 2. Details of the observations taken. *Note that geometric values are approximate for the mid time of each observing period. The V magnitudes quoted are for illustration and are based upon ephemeris calculations, not actual observations.*

Asteroid	Deduced Spectral Type	Asteroid	Deduced Spectral Type
1627 Ivar	S	14402 1991 DB	M
4179 Toutatis	S	25143 Itokawa	S(IV)
5381 Sekhmet	V	25330 1999 KV_4	C or B
5587 1990 SB	Sq	52760 1998 ML_{14}	S or Sq
6489 Golevka	Sq	66391 1999 KW_4	S(IV)
11405 1999 CV_3	Sq	101955 1999 RQ_{46}	C

Table 6: Summary of Spectral Types.

11 Figure Captions

Fig.1 1627 Ivar. Merger of the UKIRT data with that of Binzel et al (2004).

Fig.2 4179 Toutatis observed on 4 dates with phase angles from 1-80 degrees. From bottom 2000 December 01, 81 degrees; 2000 December 22, 49 degrees; 2001 January 14, 18 degrees; 2001 February 01, 0.7 degrees. Each spectrum has been offset vertically by 0.1 for clarity.

Fig.3 Ratio of K band reflectances on 2000 December 01 and 2001 February 01. There is no evidence for any systematic reddening despite the change in phase angle by 80 degrees.

Fig.4 5381 Sekmet observed with UIST on 2003 May 05. Data from the region of poor transmission shortward of 1.45μm and few clearly anomalous points have been manually removed from the data before plotting.

Fig.5 (5587) 1990 SB. UKIRT data and unpublished data by Binzel at al. Note that the Binzel spectrum has not been renormalised to 2.2μm and so has a vertical shift relative to the UKIRT spectrum below. The 'feature' at around 1.35μm in the UKIRT spectrum is an artifact of poor atmospheric cancellation.

Fig.6 6489 Golevka. CGS4 data of 1999 with data of Binzel et al (2004) overplotted. Excessively noisy data at the overlaps of the J_L/H and H/K windows have been removed.

Fig.7 (11405) 1999 CV_3 UKIRT data plus data of Binzel et al (2004).

Fig.8 (14402) 1991 DB UKIRT data and data from Binzel et al (2004).

Fig.9 Relative reflectance for the four spectra in each of two spectyral fragments. Apart from the upper spectrum in a), there is no evidence for spectral variations with rotational phase. a) J_{short} band: solid circles taken at rotational phase of 0.06 (where phase = 0 corresponds to the time of the first spectrum on 17 March and the rotation period is 12.118 hours derived from the J-band photometry and unpublished optical photometry); open squares at rotational phase of 0.26, and reflectance offset by -0.1; solid squares at rotational phase of 1.89, and reflectance offset by -0.2; open circles at rotational phase of 2.09, and reflectance offset by -0.3. b) K band: solid circles taken at rotational phase of 0.17 open squares at rotational phase of 0.35, and reflectance offset by -0.1; solid squares at rotational phase of 2.02, and reflectance offset by -0.2; open circles at rotational phase of 2.20, and reflectance offset by -0.3.

Fig 10 a) Relative reflectance spectrum of 25143 Itokawa produced by fitting overlap regions of spectral fragments, normalised to the K band spectrum between 2.15 and 2.25μm. b) Comparison of relative reflectance spectrum of 25143 Itokawa produced by fitting overlap regions of spectral fragments (filled circles) to that produced by fitting spectral fragments to broadband photometry (crosses and open circles).

Fig.11 (25330) 1999 KV_4.

Fig.12 (52760) 1999 ML_{14}.

Fig.13 (66391) 1999 KW_4 compared with the main belt object 25 Phocaea.

Fig.14 (101955) $1999RQ_{36}$.